

6. A Tectonic Stress Trajectory Map of Alaska Using Information from Volcanoes and Faults*.

By Kazuaki NAKAMURA,

Earthquake Research Institute, Univ. Tokyo, Tokyo 113,

George PLAFKER,

U. S. Geological Survey, Menlo Park Calif. 94025,

K. H. JACOB and J. N. DAVIES,

Lamont-Doherty Geological Observatory, Columbia Univ.
Palisades, N. Y. 10964.

(Received Feb. 29, 1980)

Abstract

A preliminary tectonic stress trajectory map for the Alaska region is compiled from 44 directions of maximum horizontal compression obtained from published data about post-Miocene volcanoes and late Quaternary faults. The pattern of the trajectory lines gives an averaged picture of the tectonic stress field during the late Quaternary. The pattern correlates with relative motion between the Pacific and North America plates, as judged by parallelism between the trajectory lines and direction of convergence of the two plates. Within a zone several hundred kilometers wide along the plate boundary, the mapped trajectories coincide with *P*-axes (i.e. direction of maximum principal stress, σ_1) in a three-dimensional stress system. In the eastern Bering sea and interior Alaska, *P*-axes appear to be vertical and the mapped trajectories probably represent the *B* or axes of intermediate stress (σ_2). Thus, the compressive stress in the arc area is replaced in the back-arc region by tensional stresses which are probably caused by a large-scale, deep-seated stress source. Despite this tensional stress field in the back-arc region no coherent spreading is observed there behind the Alaska Aleutian arc system. It is suggested that back-arc regions are potentially extensional but that the formation of back-arc basins depends on a mechanism other than subduction near the trench so that the space of an extending back-arc region is appropriately filled.

Introduction

A trajectory map of tectonic stress axes averaged over a geologically

* Lamont-Doherty contribution number 2934.

significant period is a simple way to portray large-scale, long-term tectonics. Usefulness of regional mapping of tectonic stress trajectories has long been advocated by workers in neotectonics (e.g. LENSEN, 1960; HUZITA, 1969; PAVONI, 1971; NAKAMURA, 1979). Regional stress data are presented here both from volcanic features, such as dike swarm patterns, and from large-scale faults. Such a map contains some information for causative mechanisms for the stress field of the crust. Also it can offer a comprehensive understanding about the type of dominant crustal deformation which occurred during the relevant period. A stress trajectory map averaged over periods long enough to be tectonically significant also provides an evaluation of short-term or transient stresses as indicated by seismic focal mechanism solutions and in situ stress or strain measurements.

NAKAMURA *et al.* (1977) obtained from Alaska 43 directions of maximum horizontal compression (MHC) averaged over the recent tens to hundreds of thousand years, 28 directions from volcanoes and 15 from faults. Geographical uniformity of the directions over a sizable area convinced NAKAMURA *et al.* (1977) that the directions of these MHC coincide with those of principal tectonic stresses, rather than local or gravitational ones. In a three-dimensional stress system, the directions of MHC can be either the maximum (compressional) or the intermediate-stress axis. In the latter case, the maximum compression is vertical. Using other evidence such as parallelism of MHC with directions of plate convergence along the Aleutian trench (MINSTER *et al.*, 1974) and geographical distribution of types of volcanoes, NAKAMURA *et al.* (1977) inferred that along the plate boundaries, mapped directions of MHC represented maximum compression and that in the back-arc region they represented intermediate-stress axes with the maximum compression vertical.

This paper presents a stress trajectory map of the Aleutian islands and continental Alaska using the results of NAKAMURA *et al.* (1977) with some modification, especially for fault data, and briefly considers its implication for tectonics of the arc and back-arc system.

Data

Most data of MHC obtained from volcanoes and of maximum horizontal shortening (MHS) from faults as presented in NAKAMURA *et al.* (1977) are used with some deletions, corrections and additions for delineating MHC trajectory lines in Fig. 3. The method for obtaining such directions is described by NAKAMURA (1977) for volcanoes and by LENSEN (1960) for faults. What we obtain from faults is the direction of MHS which can be used as an approximation to MHC (e.g. LENSEN *et al.*, 1971).

To obtain directions of MHC from volcanoes, various surface features indicating patterns of radial and parallel dikes are used. The distributions of monogenetic volcanoes as flank and post-caldera cones on composite volcanoes are the most useful features. Because dikes tend to develop in a plane defined by maximum compressive and intermediate stress axes and because dikes (by definition) are more or less vertically dipping, the surface trace of a dike is a good approximation to that of

Table 1. Probable azimuths of concentration of radial and parallel dike of Aleutian and Alaskan volcanoes.

No. ¹	Volcano ¹	Azimuth (from north) ²	Quality ³
87	Imuruk Lake	{45°W±15° 40°E±20°}	G P
88	Kookooligit Mtns.	80°W±5°	E
89	St. Michael Island	60°W±10°	G
91	Ingakslugwat Hills	90°E±20°	P
93	Nunivak Island	80°W±10°	G
96	St. Paul Island	{55°W±10° 50°E±20°}	G G
99	St. George Island	70°E±20°	G
100	Buldir	60°W±10°	P
101	Kiska	50°E±25°	VP
102	Segula	40°W±10°	G
104	Little Sitkin	65°W±15°	P
105	Cerberus	35°W±20°	P
107	Gareloi	45°W±5°	G
112	Moffett	50°W±10°	G
113	Adagdak	60°W±10°	P
114	Great Sitkin	35°W±10°	G
131	Vsevidof	65°W±20°	P
132	Recheshnoi	70°W±10°	P
133	Okmok	60°E±10°	VP
135	Bogoslof	25°W±5°	P
136	Makushin	60°W±15°	VP
138	Akutan	60°W±15°	VP
154	Dana	40°W±10°	G
165	Veniaminof	35°W±5°	E
157	Purple (Black) Peak	55°W±15°	G
158	Aniakchak	15°W±25°	P
174	Iliamna	25°W±10°	G
178	Spurr	20°W±20°	VP
186	Edgecumbe	40°E±10°	E

Data sources are given in Nakamura et al., 1977, except for Mount Cerberus Volcano (105).

¹ after SMITH and SOULE, 1973.

² Azimuth of the probable preferred orientation of dikes as obtained principally from the distribution of craters and supplementally from elongation areas and fault trends.

³ Quality of azimuths, E: excellent, G: good, P: poor, VP: very poor.

MHC of the ambient stress during its emplacement. Therefore, the general trend of a swarm of parallel dikes gives an averaged trend of MHC for the entire period of the dike activity. In the case of radial dikes, concentration into a preferred direction has the same significance as the trends of parallel dikes. These features of dikes are approximately known from the azimuthal distribution of monogenetic (flank and post-caldera) volcanoes around the main polygenetic vent (NAKAMURA, 1977).

Volcanoes

In Table 1 the MHC directions are listed which were obtained from volcanoes. They were given by NAKAMURA *et al.* (1977) except for Mount Cerberus volcano, which is described below focussing on the features related to obtaining MHC directions.

According to COATS (1959), Mount Cerberus (51°56'N, 179°35'E, No. 105 after SMITH and SOULE, 1973) is a group of post-caldera cones of a large stratovolcano forming most of the Semisopchnoi island, which is informally called here Mount Cerberus volcano. The volcano (Tertiary (?) and Quaternary) has a summit caldera and 12 younger cones including Mount Cerberus. The Crater lake-type caldera was formed after the latest glaciation. Of 12 cones shown in Fig. 1, four are considered to be late Pleistocene basaltic cones of approximately the same age as the caldera; The other 8 cones postdate the caldera.

The general location of Mount Cerberus (MC in Fig. 1) may be taken as the site of the main polygenetic vent, because it marks the most productive and latest eruption site within the caldera. However,

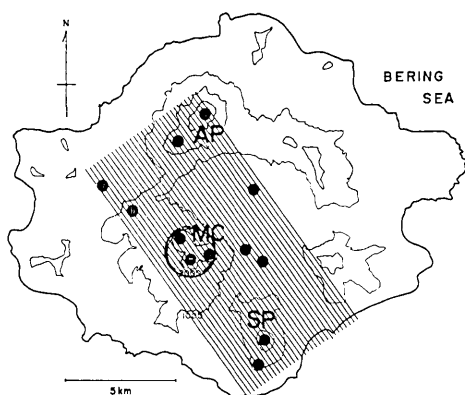


Fig. 1. Volcanoes on Semisopchnoi island, Aleutians (COATS, 1959). Shaded is the zone of crater distribution. The strike of the zone is taken as the direction of σH_{max} .
Dot: crater, MC: Mount Cerberus, the assumed polygenetic center, SP: Sugarloaf Peak. Contour interval: 1,000 ft.

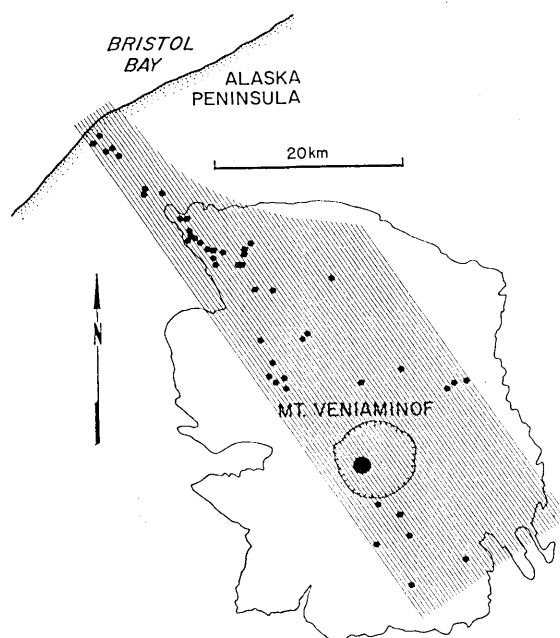


Fig. 2. Veniaminof volcano on the Alaska Peninsula. Larger dot in the caldera indicates the location of the polygenetic vent. Smaller dots are flank volcanoes.

it is not certain that Sugarloaf Peak (SP, No. 106 after SMITH and SOULE, 1973) and Anvil Peak (AP) are monogenetic. They are quite large in volume as monogenetic volcanoes and have possible satellitic volcanoes of their own. SMITH and SOULE (1973) regard Sugarloaf Peak as an independent stratovolcano (i.e. polygenetic volcano).

With these uncertainties in mind, the direction of $N35^{\circ}W \pm 20^{\circ}$ may be taken as the elongate direction of the zone of monogenetic volcanoes (ca. 11 km long and 5.5 km wide) or the preferred orientation of radial dikes of Mount Cerberus volcano. The quality is assigned as poor, on the basis of the above description. (For details of quality assignment, see NAKAMURA *et al.*, 1977, p. 102-103). The direction assigned as excellent at the volcano Veniaminof (No. 156) in the Alaska Peninsula is reproduced in Fig. 2 for comparison.

Faults

Table 2 lists data from late Quaternary faults used to draw trajectory lines in Fig. 3. This table is similar to the Table 2 of NAKAMURA *et al.* (1977) and the numbers attached to faults remain the same, except for addition of 16, 17 and 18 and deletion of 4, 9, 11, and 15.

The data in Table 2 are significantly different from the earlier

Table 2. Probable azimuths of maximum horizontal shortening (MHS) of Quaternary faults in Alaska.

Name	General trend (from north)	Sense ¹	Length (km)	MHS Azimuth (from north) ²	Quality ³	Reference ⁴
1. Fairweather	38°W	D	250	7°E	E	a
2. Totschunda	32°W	D	200	13°E	E	b
3. Denali	{east of 150°W west of 150°W	{55°W-75°E 60°E	{480 540	{30°-10°W 75°W	{E G	b
5. Hanning Bay	45°E	R	6	45°W	P	c
6. Patton Bay	37°E	R	62	53°W	G	c
7. Castle Mountain	55°E	D	45	80°W	G	d
8. McGinnis Glacier	NW	D	50	0°	G	d
10. Healy Creek	E	R	18	0°	VP	e
12. Tintina	25°-30°E	D	100	15°-20°E	G	d
13. Kaltag	65°E	D	400	70°W	G	e
14. Dall Mountain	NS-23°W	N	30	0°-23°W	VP	d,f
16. Bendeleben	EW	N	90	EW	G	g
17. Kigluaik	EW	N	65	EW	G	g
18. Bering Strait	EW	N	20+	EW	G	h

¹ D: dextral strike-slip, S: sinistral strike-slip, N: normal, R: reverse.

² Derived from strike and dominant sense of displacement.

³ Same as in Table 1.

a: PLAFKER *et al.*, 1977

b: PLAFKER *et al.*, 1978

c: PLAFKER, 1965, 1972

d: BROGAN *et al.*, 1975

e: PATTON, 1977

f: PLAFKER AND HUDSON, unpublished data

g: HUDSON and PLAFKER, 1978

h: HOPKINS *et al.*, 1974

one, however, although the result as expressed in Fig. 3 does not make much difference. The data source for the earlier table was exclusively BROGAN *et al.* (1975) for the sake of uniformity of the quality of data. In Table 2 are included other results which are indicated in the column of reference. Quality *E* (excellent) is assigned for the faults longer than 200 km, *G* (good) for those between 200 km and 10 km, and *P* (poor) for those shorter than 10 km, when the sense and the displacement of the faults during the late Quaternary are known. When the displacement during the late Quaternary is suspected, quality *VP* (very poor) is given.

The Kigluaik (17) and Bendeleben (16) faults are principal active faults of the Seward Peninsula and have large amounts of late Cenozoic dip slip displacement (HUDSON and PLAFKER, 1978). The two faults together define a normal fault system that is about 175 km long. They trend approximately east-west, are subparallel but not overlapping, and have opposite senses of displacements. Surface features indicative of

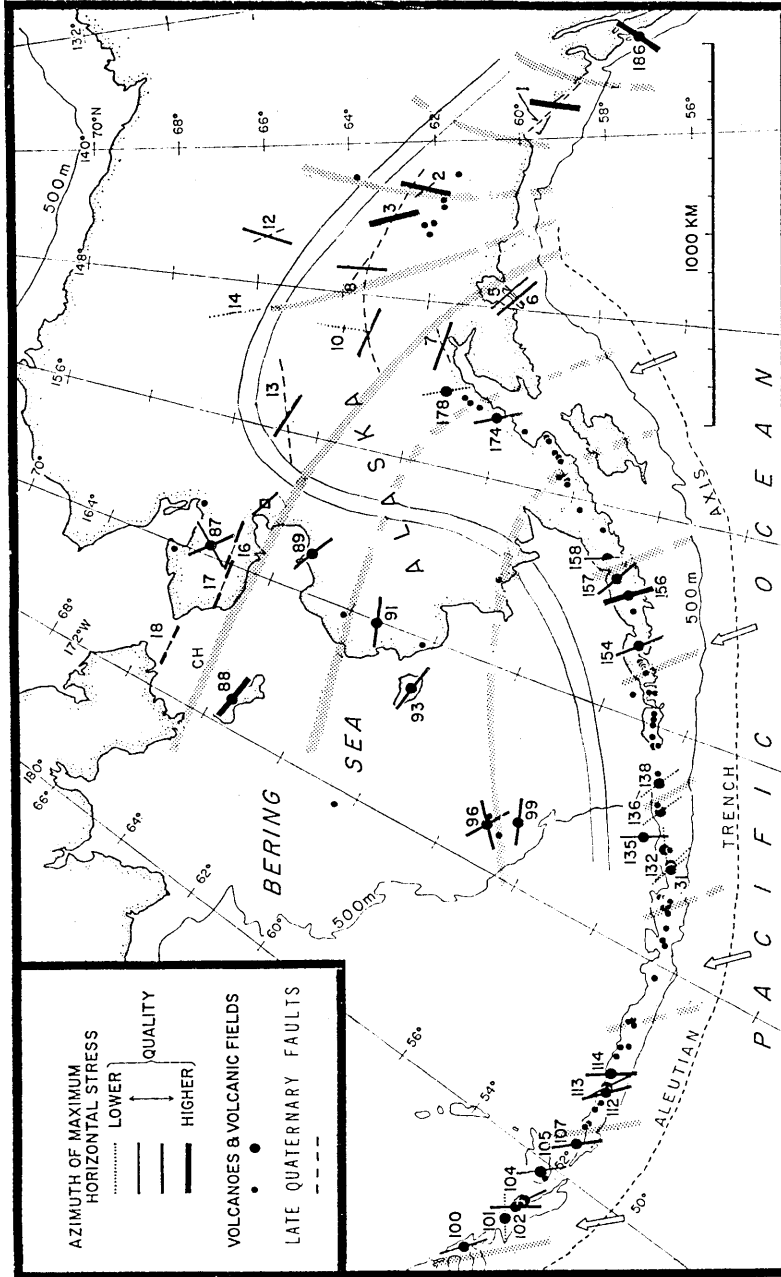


Fig. 3. Map of the late Quaternary tectonic stress trajectories of the Aleutians and Alaska. Data in Tables 1 and 2. Stress trajectories (stippled lines) represent averaged directions of MHC or $\sigma_{H_{max}}$, which can be either σ_1 or σ_2 . Sinuous double line locates approximate boundary between compressional ($\sigma_{H_{max}} = \sigma_1$) and extensional ($\sigma_{H_{max}} = \sigma_2$, $\sigma_1 = v_1$) tectonic stress fields. Open arrows: directions of motion of Pacific plate relative to North American plate (MINSTER *et al.*, 1974). Square and bar show the epicenter and B axis of an earthquake of normal fault type (SYKES and SBAR, 1974). Ch: Chirikov basin.

Holocene displacement are present, and total post-Wisconsin displacement may be several meters on the two faults.

The Bering Strait faults (18) are one out of many expressions in the Chirikov basin (Fig. 3) that the direction of MHC lies in a general E-W direction in good agreement with the Kigluaik and Bendeleben normal fault system and the N80°W-trending crater distribution on the Kookooligit mountain, St. Lawrence island (volcano No. 88 after SMITH and SOULE, 1973). In the Chirikov Basin several active faults and scarps generally trend east-westerly which are concentrated around the periphery of the basin, showing dip-slip displacements commonly with basinward sides downthrown (GRIM and McMANUS, 1970, HOPKINS *et al.*, 1974, 1976, HOPKINS, personal communication, 1977, HOWARD *et al.*, 1978). The largest lineament is the Cape York-Bering Strait fault system consisting of the Cape York fault system (80 km long), Bering Strait fault system (over 20 km long) and several other shorter parallel faults. The Bering Strait faults are described as normal faults (HOPKINS *et al.*, 1974). Others are sometimes described as rifts having dip-slip components.

The Kaltag fault (13) is reduced to *G*, because PATTON (1975) did not find evidence of modern activity along an important portion of the fault. Quality of the Donnelly Dome (9), the Healy Creek (10), and the Dall Mountain (14) faults is reduced to a lower class because of doubt regarding their activity during the late Quaternary (PLAFKER and HUDSON, unpublished data). Since the quality of the Donnelly Dome fault (9) was already VP, this fault is deleted from the Table 2.

The Ragged Mountain fault (4) is a rather unusual normal fault in that the fault plane dips only by 8 degrees and that the fault was probably formed originally as a thrust fault in the late Tertiary. It has been interpreted by TYSDAL *et al.* (1976) as recent reversal of movement due to gravity, but not to tectonic stress. For this reason, we consider that this fault should be deleted from our data.

The Shaw Creek fault (11) assigned as VP in the previous table is deleted because HUDSON *et al.* (1977) did not recognize recent tectonic displacement and suggested it is inactive. Similarly, no evidence could be found for Quaternary movement on the Kabuk-Alatna Hills fault (15) (PLAFKER and HUDSON, unpublished data) and this fault is deleted from the table.

Results and discussion

On the basis of data given in Tables 1 and 2 MHC trajectory lines are drawn as in Fig. 3. Although the trajectory map itself was not presented, most features shown in Fig. 3 were previously described

by NAKAMURA *et al.* (p. 108-109). These include (1) parallelism between the directions of MHC trajectory lines and of convergence of the Pacific and America plates along the Aleutian trench as shown by open arrows in Fig. 3, (2) the fan-shaped pattern of trajectory lines in interior Alaska with the symmetry line in the direction of the plate convergence and (3) a right-angle relation of the trajectory lines in the southeast Bering Sea. NAKAMURA *et al.* thought that these features are mostly explicable in terms of converging interaction between the Pacific and North American plates. An exception is the right-angle relations in the southeast Bering Sea, which might reflect possible east-west compression across the narrow continental connection between North America and Asia. However, the compression, if any, should not be large, because the east-west stress there is σ_2 and smaller than σ_3 (overburden) which is σ_1 . A higher density of trajectories near the southern end of the symmetry line may correspond to the strongly compressional zone of the Chugach—St. Elias Range (e.g. Perez and Jacob, 1980).

The trajectory lines of MHC along the trench appear to correspond to P -axes (σ_1) and those in the back-arc (Bering Sea and interior Alaska) region to B -axes (σ_2) as inferred by NAKAMURA *et al.* (1977). An approximate boundary between the two regions where trajectory lines represents P and B axes respectively, is also indicated in Fig. 3. Reverse faults are usually dominant in the southern forearc region, normal faults are dominant in the northern back-arc regions, respectively. The boundary is consistent with the dominance of different types of volcanoes, in respective regions: i.e. polygenetic calcalkaline volcanoes in the southern more compressive and monogenetic alkali-basaltic volcanoes in the northern tensional regions. The southern zone may be subdivided into two subparallel zones with σH_{\min} of either σ_2 or σ_3 . In the northern subzone where σH_{\min} is σ_3 , strike-slip faults are common. In the southern subzone, σH_{\min} is σ_2 as judged by the occurrence of thrust faults. Thus, there appear to exist the stress gradient across the Aleutian arc, which is also observed for other arcs (NAKAMURA and UYEDA, 1980).

Presence of an extensional tectonic region within the back-arc area of continental Alaska, has possible interesting implication for the mechanism of back-arc spreading. This back-arc region has never experienced any widespread back-arc-type spreading in recent geologic times, which is obvious from the geologic data at least for continental Alaska. Also the Aleutian basin, the oceanic portion of the Bering Sea, is supposed to be a part of old Pacific Ocean crust (Kula plate?) trapped by formation of the Aleutian Arc (COOPER *et al.*, 1976), rather than formation by

spreading in the back-arc region of the Aleutian Arc. Therefore, as discussed by NAKAMURA and UYEDA (1980), a possibility exists that in areas behind subduction zones large areas with an extensional tectonic regime almost always develop, but that this extensional tectonic regime is not necessarily resulting in active spreading and formation of *new* ocean basins. If this hypothesis holds then it follows that for a back-arc basins to form by active spreading, another enabling factor is necessary which allows the potential tensional stress fields to operate and to form basins by emplacement of new crustal material. This "enabling factor" would be the decrease of compressional stress at the trench or arc. This is essentially the same as the mechanism proposed by SCHOLZ *et al.* (1971) for formation of the Great Basin of the western U.S.. Presence of extensional tectonic regimes behind some arcs (Aegean, BERCKHEMER, 1977; southern Chile, SKEWS and STERN, 1979, Alps, ILLIES and GREINER, 1978) appears to support the possibility (NAKAMURA and UYEDA, 1980). While this decrease in stress along the boundary would well be a mechanism for back-arc spreading, a positive increase in tensional stress by some other mechanisms, such as the suction force at trenches, of the potentially active tensional stress could also be a possibility.

UYEDA and KANAMORI (1979) reviewed the problems of back-arc opening, related it to two different modes of subduction (compressive Chilean and tensional Mariana types), and proposed two alternative models to explain the two modes. The area of the present study belongs to their Chilean type. The tensional stress field behind their Chilean type of subduction boundary, such as the present area and southern Chile (SKEWS and STERN, 1979), may point to their oversimplification in that they assumed a uniform stress field in the overlying plates and related back-arc spreading directly to the difference in stress state in the subduction zone. The problem will be discussed elsewhere (NAKAMURA and UYEDA, 1980) in a wider scope.

Acknowledgements

This study was begun while K. N. was at the Department of Geophysics, Stanford University, supported by the National Science Foundation Grants HES 75-17623-A01. Helpful comments to the present study by David M. Hopkins are acknowledged. Kunihiko Shimazaki's comments to the manuscript was helpful for improving it. K. H. J. and J. N. D. received support for this study from the U. S. Department of Energy, Office of Basic Energy Sciences, under contract EY-76-S-02-3134.

References

- BERCKHEMER, H., 1977, Some aspects of the evolution of marginal seas deduced from observations in the Aegean region, Intern'l. Symp. Struct. Hist. Mediterranean Basins, 303-314.
- BROGAN, G. E., CLUFF, L. S., KORRINGA, M. K. and SLEMMONS, D. B., 1975, Active faults of Alaska, *Tectonoph.*, **29**, 73-85.
- COATS, R. R. 1959, Geologic reconnaissance of semisopochnoi island Western Aleutian Island Alaska, *U. S. Geol. Surv. Bull.*, 1028-O, 477-519.
- COOPER, A. K., MARLOW, M. S., and SCHOLL, D. W., 1976, Mesozoic magnetic lineations in the Bering Sea marginal basin, *J. Geophys. Res.*, **81**, 1916-1934.
- GRIM, M. S. and MCMANUS, D. A., 1970, A shallow seismic-profiling survey of the northern Bering sea, *Marine Geol.*, **8**, 293-320.
- HOPKINS, D. M., ROWLAND, R. W., ECHOLS, R. E. and VALENTINE, P. C., 1974, An Anvillian (Early Pleistocene) marine fauna from western Seward Peninsula, Alaska, *Quat. Res.*, **4**, 441-470.
- HOPKINS, D. M., NELSON, C. H., PERRY, R. B. and ALPHA, T. R., 1976, Physiographic subdivisions of the Chrikov Basin, northern Bering sea, *U.S. Geol. Surv. Prof. Paper*, 759-B, B1-B7.
- HOWARD, K. A. and 13 others, 1978, Preliminary map of young faults in the United States as a guide to possible fault activity, *U.S. Geol. Surv.*, Map MF-916.
- HUDSON, T., FOSTER, H. L. and WEBER, F. R., 1977, The Shaw creek fault, east central Alaska, *U.S. Geol. Surv. Circular*, 751-B, B33-B34.
- HUZITA, K., 1969, Tectonic development of southwest Japan in the Quaternary period, *J. Geosci. Osaka City Univ.*, **12**, 53-69.
- ILLIES, J. H. and GREINER, G., 1978, Rhinegraben and the Alpine system, *Geol. Soc. Amer. Bull.*, **89**, 770-782.
- LENSEN, G. J., 1960, Principal horizontal stress directions as an aid to the study of crustal deformation, *Publ. Dom. Obs. Ottawa*, **24**, 389-397.
- LENSEN, G. J. and OTWAY, P. M., 1971, Earthshift and post-earthshift deformation associated with the May 1968 Inangahua earthquake, New Zealand, *Roy. Soc. N. Z. Bull.*, **9**, 107-116.
- MINSTER, J. B., JORDAN, T. H., MOLNER, P. and HAINES, E., 1974, Numerical modelling of instantaneous plate tectonics, *Geophys. J. R. Astr. Soc.*, **36**, 541-576.
- NAKAMURA, K., 1977, Volcanoes as possible indicators of tectonic stress orientation—principle and proposal, *J. Volcanol. Geotherm. Res.*, **2**, 1-16.
- NAKAMURA, K., 1979, σH_{\max} trajectories east of Suruga trough, Japan—an effect of flexure of lithospheric plate, *Zisin*, **32**, 370-372. (in Japanese)
- NAKAMURA, K., JACOB, K. H. and DAVIES, J. N., 1977, Volcanoes as possible indicators of tectonic stress orientation—Aleutians and Alaska, *Pageoph.*, **115**, 87-112.
- NAKAMURA, K. and UYEDA, S., 1980, Stress gradient in arc and backarc regions and plate subduction, *J. Geophys. Res.*, **85**. (in press)
- PATTON, W. W. Jr., 1975, New information on the Kaltag fault, *U. S. Geol. Surv. Circular*, **722**, 43.
- PAVONI, N., 1971, Recent and late Cenozoic movements of the earth's crust, *Roy. Soc. New Zealand Bull.*, **9**, 7-17.
- PEREZ, O. J. and JACOB, K. H., 1980, Tectonic model and seismic potential of the eastern Gulf of Alaska and Yakataga seismic gap., *J. Geophys. Res.* (in press)
- PLAFKER, G., 1965, Tectonic deformation associated with the 1964 Alaska earthquake, *Science*, **148**, 1675-1687.
- PLAFKER, G., 1972, Alaskan earthquake of 1964 and Chilean earthquake of 1960: implications for arc tectonics, *J. Geophys. Res.*, **77**, 901-925.
- PLAFKER, G., HUDSON, T. and RICHTER, D. H., 1977, Preliminary observations on late Cenozoic displacements along the Totschunda and Denali fault systems, *U. S. Geol. Surv. Circular*, 751-B, B67-B69.

- PLAFKER, G., HUDSON, T., BRUNS, T. and RUBIN, M., 1978, Late Quaternary offsets along the Fairweather fault and crustal plate interactions in southern Alaska, *Can. J. Earth Sci.*, **15**, 805-806.
- SCHOLZ, C., BARAZANGI, M. and SBAR, M. L., 1971, Late Cenozoic evolution of the Great Basin, western United States, as an ensialic interarc basin, *Geol. Soc. Amer. Bull.*, **82**, 2979-2990.
- SKEWES, M. A. and C. R. STERN, 1979, Petrology and geochemistry of alkali basalts and ultramafic inclusions from the Palei-Aike volcanic field in southern Chile and the origin of the Patagonian plateau lavas, *J. Volcanol. Geotherm. Res.*, **6**, 3-25.
- SMITH, R. L. and SOULE, C. E., 1973, Western Alaska and Bering Sea Islands, Alaska Peninsula and the Aleutian Islands and Range in Data Sheets of the Post-Miocene volcanoes of the world with index maps (IAVCEI, Rome).
- SYKES, L. R. and SBAR, M. L., 1974, Focal mechanism solutions of intraplate earthquakes and stresses in the lithosphere, in *Geodynamics of Iceland and north Atlantic area*, edited by L. Kristjansson, 207-224, D. Riedel, Hingham, Mass.
- TYSDAL, R. G., HUDSON, T. and PLAFKER, G., 1976, Surface features and recent movement along the Ragged Mountain fault, South-central Alaska, *U.S. Geol. Surv. Misc. Field Studies*, Map MF-782.
- UYEDA, S. and KANAMORI, H., 1979, Back-arc opening and the mode of subduction, *J. Geophys. Res.*, **84**, 1049-1061.

6. 火山と断層の情報から作ったアラスカのテクトニック主応力線図

地震研究所 中村 一明

アメリカ地質調査所 George PLAFKER

コロンビア大学ラモント・ドアティ地質研究所 Klaus H. JACOB

John H. DAVIES

中新世以新の火山と第四紀後期の断層の資料から求められた44ヶの $\sigma_{H_{max}}$ 方位に基づいて、アラスカ地域のテクトニック主応力線図を画いた。この主応力線図のボタンは第四紀後期のテクトニック応力場の平均的な像を与える。太平洋プレートとの境界付近のボタンは σ_1 軌跡を与えプレート相対運動に起因すると思われる。したがって最近数百万年間のボタンをもあらかずとみられる。ベーリング海およびアラスカ大陸内部では $\sigma_{H_{max}}$ は σ_2 で σ_0 が σ_1 とみられる。それ故、プレート境界部の圧縮応力場は数百 km 以内で、別の原因をもつ引張り応力場にかわっている。この引張り応力場地域は最近地質時代に縁海を生ずるような拡大を行っていない。他の弧地域の例を考慮すると、サブダクションに常に伴って背後に引張り応力場が生じ、何か別の原因でこの応力場がより活動的になると縁海を生ずるような拡大が起こる、という可能性が示唆される。